Spectroscopic and Computational Studies of Perfluorophenyl and Perfluoro-2-naphthyl Nitrenes in Shpolskii Matrixes

B. Kozankiewicz* and I. Deperasiñska
Institute of Physics, Polish Academy of Sciences, Al. Lotników 32/46, 02-668 Warsaw, Poland

H. B. Zhai, Z. Zhu, and C. M. Hadad*
Department of Chemistry, The Ohio State University, Columbus, Ohio 43210

Received: January 19, 1999; In Final Form: May 10, 1999

Fluorescence and fluorescence excitation spectra of the photolysis products of perfluorophenyl azide and perfluoro-2-naphthyl azide in *n*-hexane and *n*-heptane at 5 K were recorded. The spectra with (0,0) transitions at 18 800 and 18 300 cm^{-1} were assigned to perfluorophenyl nitrene and perfluoro-2-naphthyl nitrene, respectively. A narrow spectrum with a (0,0) transition at 17 300 cm^{-1} was attributed to the aryl aminyl radical derived from perfluoro-2-naphthyl nitrene formed by abstraction of a hydrogen atom from the surrounding solvent matrix. The experimental results are consistent with calculations using semiempirical, B3LYP, and CASSCF/CASPT2 methods.

I. Introduction

Nitrenes are among the most interesting and important intermediates in organic chemistry.[1] Their chemistry also has many practical applications which include both industrial processes[2] and the photoaffinity labeling of biological macromolecules.[3]

Aryl nitrenes are usually generated upon heat- or light-induced extrusion[1] of molecular nitrogen from the corresponding aryl azides. In solution at ambient temperature, singlet aryl nitrenes have nanosecond lifetimes[4] and their lower energy spin isomers, triplet nitrenes, are short-lived compounds which decay on the microsecond time scale.[1,5] High-resolution spectroscopy of nitrenes at ambient temperature is problematic as their concentration is both small and rapidly decaying. In a cryogenic matrix, friction greatly restricts molecular motion and effectively eliminates bimolecular reactions of aryl nitrenes. The low-temperature conditions also inhibit most intramolecular reactions. Thus, it is possible to produce an easily detectable concentration of triplet nitrenes and to study the same sample for several days, as long as the matrix is kept frozen.[6]

In the present work, we report experimental and theoretical investigations of the intermediates produced upon photolysis of perfluorophenyl azide and perfluoro-2-naphthyl azide dispersed in Shpolskii matrixes[6d] of *n*-hexane and *n*-heptane at 5 K. Polyfluorination of the aromatic ring raises the barrier to molecular rearrangement of the singlet nitrenes.[5] Consequently, both perfluorophenyl nitrene (C_6F_5N, PFPN) and perfluoro-2-naphthyl nitrene ($C_{10}F_7N$, PFNN) relax efficiently to their triplet ground state T_0 at low temperatures.[6,7]

Triplet phenyl nitrene (^{3}PN) is quite light sensitive.[6] Brief photolysis of ^{3}PN efficiently converts the nitrene to a didehydroazepine (ketenimine), and the fluorescence of ^{3}PN is quite weak. Dunkin and Thomson have shown that matrix-isolated ^{3}PFPN does not photoisomerize readily.[8] Thus, the fluorescence intensities of perfluorinated aryl nitrenes are much stronger than those of their nonhalogenated counterparts.[6] We have concentrated most of our current efforts on PFNN and its reaction products, which have been previously studied[7] at ambient temperatures. PFPN was studied for comparison purposes because its spectral properties at low temperature and ambient temperature are known.[5,6] In addition, semiempirical[6] and ab initio[9,10] molecular orbital calculations of the electronic transition energies are feasible for PFPN and easily related to those of the parent system phenyl nitrene (PN, C_6H_5N). Calculations on PFNN are more difficult with very accurate methods, so with appropriate calibration, we will explore these computational methods in order to understand the experimental spectra of the PFNN system.

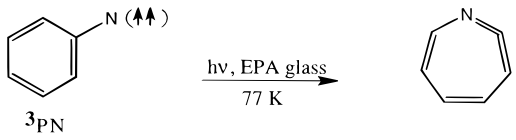

Photolysis of perfluoro-2-naphthyl azide in low-temperature Shpolskii hydrocarbon matrixes leads to two fluorescing intermediates. We will provide arguments that one of these species can be associated with a triplet nitrene (^{3}PFNN) and the second species with an aryl aminyl radical obtained when the triplet nitrene abstracts a hydrogen atom from the surrounding matrix.

II. Experimental Methods

Materials. Perfluorophenyl and perfluoro-2-naphthyl nitrenes (PFPN[6,11] and PFNN[7]) were generated by photolysis of the corresponding azides (perfluorophenyl azide and perfluoro-2-naphthyl azide) dissolved in frozen *n*-hexane, *n*-heptane, and perfluoro-*n*-hexane matrixes at a concentration of 10^{-3} M. Merck Uvasole *n*-hexane and *n*-heptane and Fluka perfluoro-*n*-hexane (purum, mixture of isomers) were used without further purification.

Fluorescence Spectroscopy. Frozen samples were obtained by rapid cooling from room temperature to 5 K in order to isolate azide precursors in substitutional sites of the matrix. The 366 nm line of an HBO 200 mercury lamp was isolated with the aid of appropriate filters and used to photolyze the sample. The photolysis process was monitored by following the increase in the intensity of the nitrene fluorescence. The intensity of nitrene fluorescence increased during the first 5 min of illumina-

* Corresponding author. E-mail: kozank@ifpan.edu.pl. Fax: (+48-22) 8430926.

10.1021/jp9902304 CCC: $18.00
Published on Web 06/10/1999

tion and was constant at longer irradiation times. On the basis of this observation, we were not able to estimate the extent of azide decomposition. Samples were annealed overnight, in the dark, by slowly raising the temperature from 5 K to about 100 K. The samples were cooled again to 5 K the next day.

Fluorescence spectra were obtained by promoting the nitrenes to their excited triplet states, T_n, by using the same 366 nm line. Alternatively, nitrenes were promoted directly to the lowest excited triplet state, T_1, by using a pulsed Lambda Physik FL1001 dye laser pumped with an LPX100 excimer laser (308 nm). The spectra were detected at a right angle with respect to the direction of the exciting light via a 0.25 cm Jarrel-Ash monochromator and an EMI 9659 photomultiplier cooled to −20 °C. Photon counting techniques were used in the case of continuous wave (cw) mercury lamp excitation experiments, whereas an analog sampling technique with a Stanford Research SR250 boxcar averager was employed in the case of pulsed laser excitation. Fluorescence excitation spectra were obtained with a Lambda Physik FL1001 dye laser system and monitoring the intensity of the strong (0,0) fluorescence transition, or of less intense vibrational bands, separated with the aid of a monochromator. During these experiments Coumarin 307 was used as a lasing dye between 490 and 540 nm and Coumarin 153 between 530 and 590 nm.

Fluorescence decays were detected either by "time-correlated" single-photon counting methods or by discrete sampling. In the former case, samples were excited by 320 nm laser pulses (of some picosecond duration) obtained as the second harmonic of a Coherent 700 dye laser (lasing on DCM) pumped by a mode-locked Antares 76-YAG laser. Start and stop signals were provided by an avalanche photodiode and a microchannel plate photomultipier (Hamamatsu R28090-07), respectively. The time resolution of this setup is about 50 ps. In the latter case, samples were excited with 337 nm pulses (of 1 ns duration) of a homemade nitrogen laser and detected using the previously mentioned photomultiplier and the boxcar averager.

Computational Techniques. Geometry optimizations were obtained with the Hyperchem[12] and the Gaussian 94[13] software packages. All stationary points were verified by vibrational frequency analyses. However, zero-point vibrational energies are not included in the relative energies in order to make comparisons with CASSCF energies. (However, inclusion of ZPE corrections changes the absolute energies by, at most, ∼1.5 kcal/mol.) Some geometries were obtained at the AM1 level with the AMPAC program.[14]

Electronic excitation energies were obtained with INDO/S and CASSCF/CASPT2 methods using the Zindo[15] and MOLCAS[16] programs, respectively. In the INDO/S calculations, the p−p interaction factor was set to 0.64 for triplet states and to 0.585 for singlet and doublet states. Density functional theory calculations were done with the hybrid B3LYP[17] method using the standard 6-31G(d) basis set.[13]

For the CASSCF/CASPT2 calculations on ^{3}PFPN, the active space (12 electrons in 12 orbitals) was chosen to provide a reasonably balanced weighting of the reference wave function for the different excited states. Contracted ANO basis sets for C, N, and F (4s3p1d quality) were used. The basis set for H was 2s1p. Six b_1 and two a_2 π orbitals as well as two a_1 and two b_2 in-plane (σ) orbitals were used in the active space.

III. Results

Fluorescence and Fluorescence Excitation Spectra of the Photolysis Product of Perfluorophenyl Azide. The fluorescence and fluorescence excitation spectra of perfluorophenyl nitrene (PFPN) in *n*-hexane at 5 K are shown in Figure 1. The (0,0) transition bands of both spectra coincide at 18 800 cm^{-1}. Both spectra are broad with weak vibrational components and have their maxima approximately 410, 820, 1210, 1590, and 2000 cm^{-1} removed from the (0,0) transition frequency. The shape and large Stokes shift of both spectra suggest that there is a considerable change of the geometry of PFPN in the excited state, compared to the T_0 ground state. A large change in geometry is predicted by theory upon $T_0 \rightarrow T_1$ excitation of triplet phenyl nitrene.[9] The shape of the spectrum and the frequency position of the band maxima observed in *n*-hexane at 5 K are in very good agreement with the fluorescence and absorption spectra of PFPN observed in ether−pentane−alcohol (EPA) matrixes at 77 K.[6]

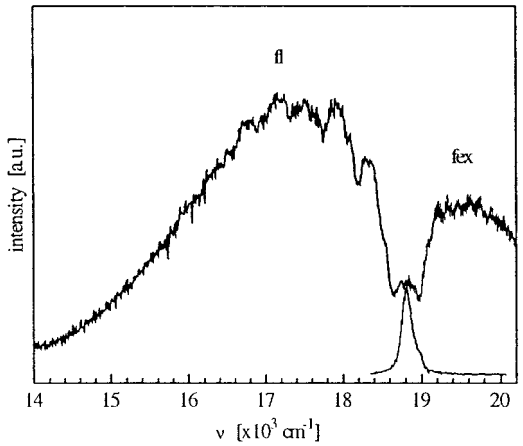

Figure 1. Fluorescence (fl) and fluorescence excitation (fex) spectra of PFPN in *n*-hexane at 5 K. The fl spectrum was obtained by excitation at 27 325 cm^{-1} (366 nm line) and the fex spectrum by observation at 16 700 cm^{-1}.

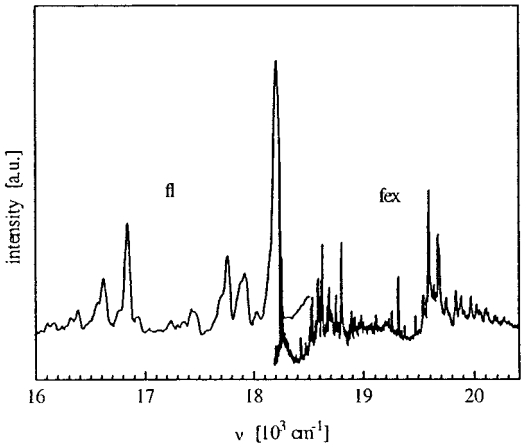

Figure 2. Fluorescence (fl) and fluorescence excitation (fex) spectra of PFNN in *n*-hexane at 5 K. The fl spectrum was obtained with excitation at 19 597 cm^{-1}. The fle spectrum in the spectral range of 18 230 to 18 870 cm^{-1} was obtained by observation at 16 905 cm^{-1} and in the spectral range 18870−20400 cm^{-1} by observation at 18 835 cm^{-1}.

The fluorescence decay, observed at 17 250 cm^{-1}, is approximately a single-exponential decay and has a decay time of 16 ns.

Fluorescence and Fluorescence Excitation Spectra of the Photolysis Product of Perfluoro-2-naphthyl Azide. *1. In n-Hexane Shpolskii Matrix.* Fluorescence and fluorescence excitation spectra of triplet PFNN in an *n*-hexane matrix at 5 K are shown in Figure 2. The spectra are composed of narrow

TABLE 1: Vibrational Frequencies (cm^{-1}) in the Fluorescence and Fluorescence Excitation Spectra of PFNN at 5 K in Different Hydrocarbon Matrixes[a]

n-Hexane	
fluorescence spectrum (maximum of the 0,0 origin at 18 270 cm^{-1})	fluorescence excitation spectrum (maximum of the 0,0 origin at 18 279 cm^{-1})
178	176
	267
287	292
	352
	371
	427
454	
	506
524	523
	1039
	1314
1373	1398
1590	

n-Heptane	
fluorescence spectrum (maximum of the 0,0 origin at 18 290 cm^{-1})	fluorescence excitation spectrum (maximum of the 0,0 origin at 18 281 cm^{-1})
	279
297	291
	319
455	
1373	
1591	

[a] The samples were annealed overnight at 100 K.

TABLE 2: Vibrational Frequencies (cm^{-1}) in the Fluorescence and Fluorescence Excitation Spectra of an Intermediate Identified with Perfluoro-2-naphthyl Aminyl Radical in Different Hydrocarbon Matrixes at 5 K[a]

n-Hexane[b]	
fluorescence spectrum (maximum of the 0,0 origin at 17366/17240 cm^{-1})	fluorescence excitation spectrum (maximum of the 0,0 origin at 17381/17248 cm^{-1})
301/307	301/305
386/394	390/397
	534/544
	605/602
689/700	692/699
- - -/790	778/794
	1323/1342
1341/1367	1370/1384
	1434/1443
	- - -/1556
1626/1623	

n-Heptane	
fluorescence spectrum (maximum of the 0,0 origin at 17 305 cm^{-1})	fluorescence excitation spectrum (maximum of the 0,0 origin at 17 324 cm^{-1})
302	304
391	393
	539
	695
1348	1329
	1381
	1443
	1553
1615	

[a] The spectra were recorded after the samples were annealed overnight at 100 K. [b] Data are given for the two sites presented in parts a and b of Figure 3.

vibrational lines with a (0,0) transition close to 18 280 cm^{-1} for both fluorescence (fl) and fluorescence excitation (fex). In the fluorescence spectrum, the width of all vibrational lines is limited by the spectral resolution of our apparatus. The vibrational frequencies are collected in Table 1.

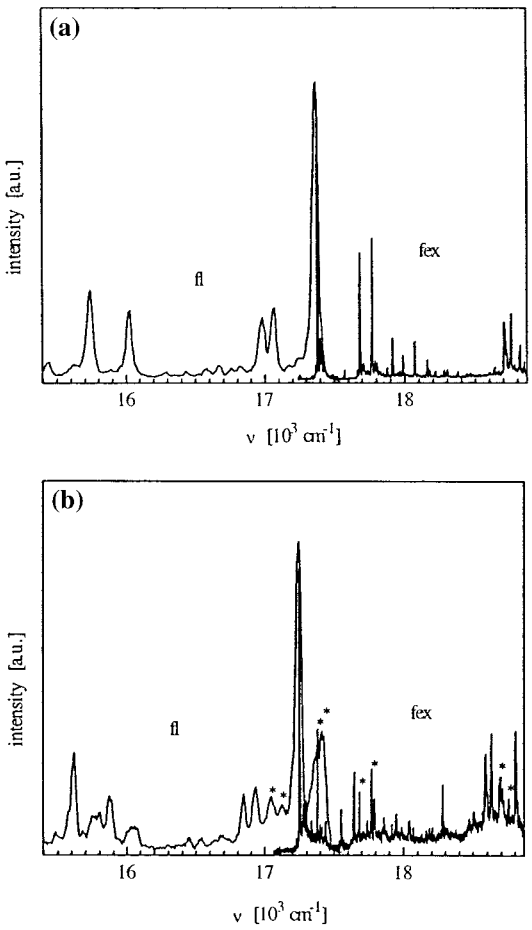

Figure 3. Fluorescence (fl) and fluorescence excitation (fex) spectra of a species identified as the perfluoro-2-naphthyl aminyl radical in *n*-hexane at 5 K. (a) The fl spectrum was obtained by excitation at 18 755 cm^{-1}, while the fex spectrum was obtained by observation at 15 735 cm^{-1}. (b) The fl spectrum was obtained by excitation at 18 805 cm^{-1}, and the fex spectrum was obtained by observation at 15 600 cm^{-1}. Lines in part b which are marked by * belong to the site contributing to the spectra of part a.

A close inspection of the (0,0) transition region of the fluorescence excitation spectrum reveals several narrow lines. Before annealing, the most intense lines are located at 549.3, 548.1, 547.9, and 547.5 nm; after annealing, new lines are observed at 546.9, 546.6, and 546.1 nm. These lines can be attributed to triplet PFNN in different matrix sites because a similar pattern of narrow lines accompanies each vibrational component of the fluorescence excitation spectrum.

After annealing, the fluorescence and fluorescence excitation spectra are modified. Various bands shift to new positions (as indicated above); however, a new spectral band is produced which is observed at lower energy. The spectra are doubled as shown in parts a and b of Figure 3. In the fluorescence excitation spectrum, the frequencies of the (0,0) transition are at 17 248 and 17 381 cm^{-1}. Each of these lines is accompanied by several lines of weaker intensity, which can be assigned to the same species in different sites of the matrix. Vibrational frequencies of this new species observed in the fluorescence and fluorescence excitation spectra are listed in Table 2.

The fluorescence decay of triplet PFNN in *n*-hexane at 5 K, observed at the maximum of the (0,0) transition at 18 280 cm^{-1},

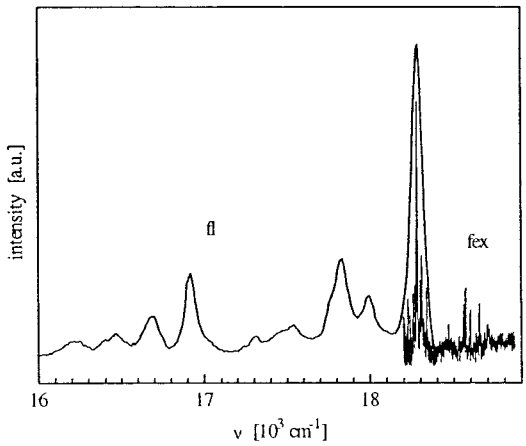

Figure 4. Fluorescence (fl) and fluorescence excitation (fex) spectra of PFNN in *n*-heptane at 5 K. The fl spectrum was obtained by excitation at 27 320 cm^{-1}, while the fex spectrum was obtained by observation at 17 800 cm^{-1}.

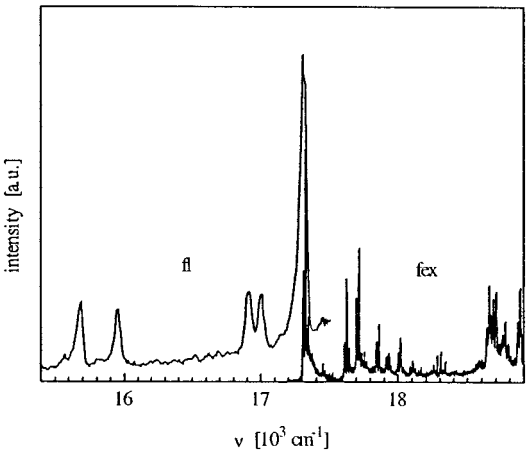

Figure 5. Fluorescence (fl) and fluorescence excitation (fex) spectra of a species identified as perfluoro-2-naphthyl aminyl radical in *n*-heptane at 5 K. The fl spectrum was obtained by excitation at 18 710 cm^{-1}, and the fex spectrum by observation at 15 680 cm^{-1}.

was found to be nonexponential. Fitting of the decay to a two-exponential function led to component decay times of 4 and 50 ns.

2. In n-Heptane Shpolskii Matrix. The fluorescence and fluorescence excitation spectra of PFNN in *n*-heptane at 5 K are shown in Figure 4, and the corresponding frequencies of the vibrational components are listed in Table 1. The spectral behavior is similar to that in *n*-hexane. In this system, a new intermediate is observed after annealing the matrix. Fluorescence and fluorescence excitation spectra of this intermediate (with (0,0) transitions at 17 305 and 17 324 cm^{-1}, respectively) are shown in Figure 5. The frequencies are listed in Table 2.

Computational Studies. The triplet perfluorophenyl nitrene (^{3}PFPN) system was studied with CASSCF/CASPT2 methods to give the results shown in Table 3. It was not possible to apply these methods to perfluoro-2-naphthyl nitrene (^{3}PFNN) due to its much larger size. Therefore, semiempirical methods were used to compute the transition energies and the oscillator strengths in both of these larger systems. To gauge the accuracy of the semiempirical methods with ^{3}PFNN, they were also applied to triplet phenyl nitrene (^{3}PN) and ^{3}PFPN and then compared to the CASSCF/CASPT2 results.[10b] The results of INDO/S calculations on triplet PFPN and PFNN are presented in Tables 3 and 4, respectively.

TABLE 3: Calculated Vertical Electronic Transitions of ^{3}PFPN (C_6F_5N)[a]

states	CASSCF eV	CASPT2 eV (cm^{-1})	CASSCF *w*	CASSCF *f*	exptl[b] eV (cm^{-1})	INDO/S eV (cm^{-1})
T_0			0.67			
T_1	3.28	2.64 (21 294)	0.66	0.001	2.5 (20 200)	2.36 (18 995)
T_2	3.46	3.11 (25 085)	0.66	0.008	3.1 (25 000)	3.91 (31 538)
T_3	4.51	4.04 (32 586)	0.67	0.012	4.0 (32 300)	3.98 (32 102)
T_4	6.57	4.22 (34 038)	0.62	0.046	4.4 (35 500)	4.51 (36 377)
T_5	4.83	4.53 (41 701)	0.66	0.001		

[a] The optimized B3LYP/6-31G(d) geometry was used for the CASSCF/CASPT2 calculations, and the optimized AM1 geometry was used for the INDO/S calculations. The CASSCF active space is (12,12), and the orbitals which were used are described in the Experimental Methods section. The basis set is a contracted ANO for C, N, and F (4s3p1d) and H (2s1p). *w* is the weight of the CASSCF wave function, and *f* is the calculated oscillator strength. [b] The vertical experimental values are taken from ref 6.

TABLE 4: Vertical Excitation Energies (cm^{-1}) from the Ground Electronic State to Four Electronically Excited States of Triplet PFNN ($C_{10}F_7N$)[a]

states	INDO/S cm^{-1} (osc. str.)	exptl (this work) cm^{-1} (adiabatic)
T_0		
T_1	17 416 (0.005)	18 280
T_2	27 533 (0.340)	
T_3	41 297 (0.000)	
T_4	48 543 (0.001)	

[a] Calculated oscillator strengths are listed in parentheses. The AM1 geometry was used. The experimental value is the average of the experimental transition energy (0,0 band) which was observed in *n*-hexane and *n*-heptane at 5 K.

The lowest energy transition of triplet phenyl nitrene in an EPA glass at 77 K[6] was discovered in 1986 by Leyva, Platz, Persy, and Wirz (LPPW). These workers assigned the transition with the aid of PPP SCF CI calculations and proposed that the weak long-wavelength band of triplet phenyl nitrene and the related band of triplet perfluorophenyl nitrene are due to $n_y \rightarrow \pi^*$ and $\pi \rightarrow n_y$ transitions. In their coordinate system, n_y is a singly occupied π orbital in the plane of the aromatic ring and is not in conjugation with the orthogonal delocalized π framework.

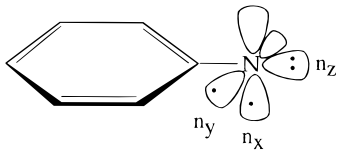

The long-wavelength transitions of triplet phenyl nitrene and perfluorophenyl nitrene (^{3}PFPN) were confidently assigned as $T_0 \rightarrow T_1$ transitions by LPPW by the observation of fluorescence with (0,0) bands at approximately 20 000 cm^{-1} (2.48 eV) and 18 500 cm^{-1} (2.29 eV), respectively.

Kim, Hamilton, and Schaefer (KHS)[9] studied the phenyl nitrene system with the aid of CISD calculations with a DZP basis set. In accord with the semiempirical study of LPPW, KHS concluded that the longest wavelength transition ($T_0 \rightarrow T_1$) of triplet phenyl nitrene corresponds to the promotion of an electron from the aromatic π system "(the highest doubly occupied orbital) to the n_x (higher singly occupied) orbital on nitrogen", which is orthogonal to the plane of the aromatic ring. The

calculated (CISD + Q/ DZ + d) adiabatic transition energy of 18 600 cm^{-1} (2.31 eV, 539 nm) was in agreement with the spectrum reported by LPPW. It is important to note that KHS predict that the T_1 state is puckered, with a barrier to planarity of 8000 cm^{-1} (~1 eV) at this level of theory.

Gritsan, Zhu, Hadad, and Platz (GZHP)[18] have recently computed the vertical excitation energies for triplet phenyl nitrene by using CASSCF/CASPT2 methods. The first calculated vertical excited state (T_1) is at 23 100 cm^{-1} (2.87 eV, 432 nm) which is at slightly higher energy than the broad, unstructured band observed to ~500 nm in an EPA matrix.[6] The difference in excitation energy between theory and experiment may be due to the geometry change between T_0 and T_1, as described by KHS.[9] This vertical transition mainly consists of the promotion of an electron from a doubly occupied π orbital to the highest singly occupied n orbital. Overall, the CASSCF/CASPT2 excitation energies and oscillator strengths reproduce the experimental spectrum very well.

A CASSCF/CASPT2 analysis of triplet PFPN has been performed (see Table 3) in a manner similar to that described by Gritsan et al.[18] for the parent phenyl nitrene system. This level of theory predicts that the vertical $T_0 \rightarrow T_1$ transition of ^{3}PFPN will be near 21 294 cm^{-1} (470 nm). As with the parent ^{3}PN, the predicted excitation energy for ^{3}PFPN is slightly higher (2.64 eV) than the observed (2.5 eV) maximum absorption in an EPA matrix. The rest of the calculated (vertical) excitation energies and relative transition moments are in good agreement with the experimental band maxima in the spectra.

The $T_0 \rightarrow T_1$ transition for triplet PFPN is due to two major configurations. They involve the promotion of an electron from the doubly occupied π orbital (a_2) to the singly occupied π (b_1) orbital (57%) and from the singly occupied π (b_1) orbital to the unoccupied π^* (a_2) orbital (19%). The nature of this transition is consistent with that predicted for triplet phenyl nitrene by GZHP.[18] The calculated oscillator strength is very small, and it is consistent with the very weak absorbance. According to the present experimental observations, the (0,0) emission band of ^{3}PFPN is at 18 800 cm^{-1} which is very similar to that observed in an EPA matrix (18 500 cm^{-1}).[6] On the basis of the CASPT2 calculations and the observations in the EPA matrix, we confidently assign the recorded 18 800 cm^{-1} emission as the $T_0 \rightarrow T_1$ transition of ^{3}PFPN.

As can be seen by inspection of Table 3, the INDO/S method predicts vertical $T_0 \rightarrow T_1$ transition energies of ^{3}PFPN that are lower in energy than that observed by matrix spectroscopy. The oscillator strength of the $T_0 \rightarrow T_1$ transition was predicted to be very small (nearly zero), but this transition is not forbidden by virtue of its symmetry. Thus, INDO/S and CASSCF/CASPT2 predict similar $T_0 \rightarrow T_1$ transition energies which are in agreement with the observed (0,0) emission and low oscillator strength of this band.

As mentioned previously, CASSCF/CASPT2 calculations of triplet perfluoronaphthyl nitrene (^{3}PFNN) are not feasible. Thus, only INDO/S results (Table 4) were obtained. By analogy to ^{3}PFPN, we use the INDO/S prediction of a weak transition at 17 416 cm^{-1} to assign the band at 18 280 cm^{-1} (obtained by photolysis of perfluoro-2-naphthyl azide) to the (0,0) band of the $T_0 \rightarrow T_1$ transition of ^{3}PFNN.

The nonexponential decay of the fluorescence of PFNN reflects the triplet state origin of the emitting T_1 state. In triplet states, three spin sublevels can be depopulated to the singlet manifold by different intersystem crossing rates which are faster than the spin−lattice relaxation, observed previously for carbenes.[19]

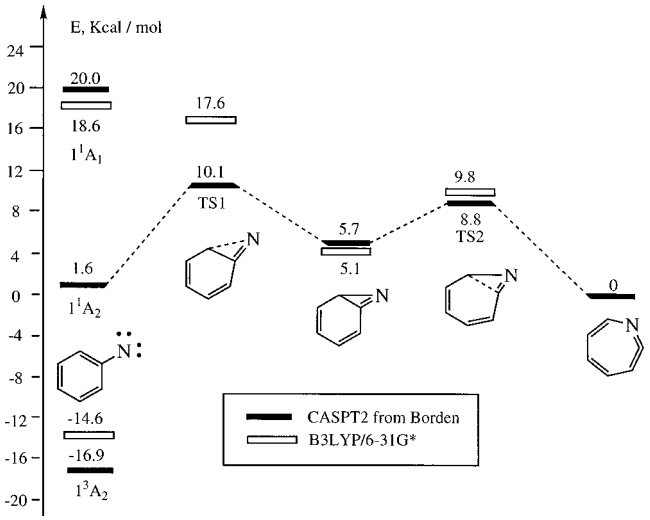

Figure 6. Potential energy surface of triplet phenyl nitrene and related species calculated by the CASPT2 and B3LYP/6-31G(d) methods.

Perfluoro-2-naphthyl Aminyl Radical. It is important to identify the reaction product which appeared in the sample containing PFNN after the annealing procedure (when the temperature rose overnight to about 100 K). This product has its (0,0) transition around 17 300 cm^{-1}. We considered two possible carriers of this transition. One possibility is a radical which results from the reaction of PFNN with the solvent matrix. The second possibility is a ketenimine created by rearrangement of the aromatic ring.

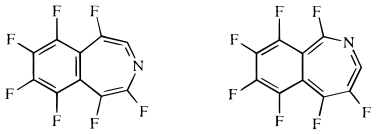

A **B**

Let us first consider the latter possibility. The existence of two ketenimines $C_{10}F_7N$ (**A**) and $C_{10}F_7N$ (**B**) at low temperature was suggested by Zhai and Platz[7] by analogy to the work of Dunkin and Thomson with 1- and 2-naphthyl nitrene.[8]

To make a meaningful comparison of the relative energies of triplet nitrenes and ketenimines, the potential energy surface (PES) of C_6H_5N was calculated at the B3LYP/6-31G(d) level of theory and compared to a higher level (CASPT2) so as to gauge the reliability of methods that could be applied to PFNN (Figure 6).

The calculations of Karney and Borden using the CASSCF/CASPT2 methods[10b] with a triple-ζ basis set (Figure 6) indicate that singlet phenyl nitrene isomerizes over a barrier of 9.2 kcal/mol to form an azirine which will rapidly ring open to form 1,2-didehydroazepine, a ketenimine. The ketenimine is lower in energy by 1.6 kcal/mol than singlet PN, but it is substantially higher in energy than triplet PN. The B3LYP/6-31G(d) method gives the same ordering of intermediates. CASPT2 and B3LYP/6-31G(d) levels predict that ^{3}PN is 16.9 and 14.6 kcal/mol, respectively, lower in energy than the corresponding ketenimine. The B3LYP calculations underestimate this gap by 2.3 kcal/mol, relative to the CASPT2 results. But qualitatively, similar results are obtained with the different methods. (We should note that the energy difference between the $^1A_2$ and $^3A_2$ states at the B3LYP/6-31G(d) level is 7.9 kcal/mol and is significantly lower than the CASPT2 value.)

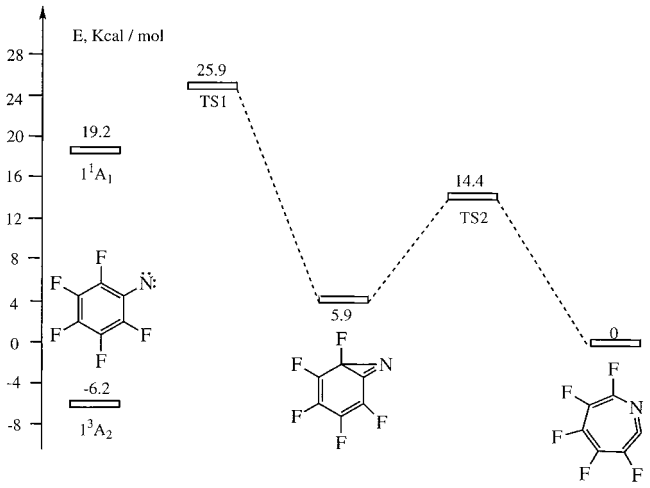

Figure 7. Potential energy surface of PFPN (C_6F_5N) and related species calculated by the B3LYP/6-31G(d) method.

The PFPN (C_6F_5N) potential energy surface was also calculated with the B3LYP/6-31G(d) method[21] (Figure 7). The B3LYP/6-31G(d) calculations predict that ^{3}PFPN is 6.2 kcal/mol lower in energy than the corresponding ketenimine. Also, these calculations predict that the azirine derived from PFPN is in a deep potential energy well, and this intermediate has been detected by Morawietz and Sander using matrix-IR spectroscopy.[22]

B3LYP calculations are feasible for the PFNN potential energy surface, and the results are shown in Figure 8.[20] Two possible ketenimines, **A** and **B**, can be formed by isomerization of PFNN. Ketenimine **A** still retains an aromatic benzenoid ring, but the other ketenimine isomer (**B**) loses aromaticity. Ketenimine **A** is preferred over the **B** isomer by 10.1 kcal/mol at the B3LYP/6-31G(d) level. We also predict that there is a large activation barrier (E_a > 20 kcal/mol) for formation of either perfluoronaphthyl azirine via TS1 or TS3 (Figure 8), and the formation of the more stable ketenimine **A** proceeds through the higher activation barrier. Thus, based on these potential energy surfaces, it seems very unlikely that ^{3}PFNN will isomerize thermally to either ketenimine **A** or **B** when the temperature of the matrix is increased from 5 to 100 K. (Since the annealing was done in the dark, we can also preclude a photochemical transformation.)

TABLE 5: INDO/S Vertical Excitation Energies (cm^{-1}) from the Ground Electronic State to Four Electronically Excited States of Singlet Ketenimines A and B ($C_{10}F_7N$)[a]

	INDO/S, cm^{-1}	
states	ketenimine **A**	ketenimine **B**
S_0		
S_1	20 805 (0.024)	18 953 (0.061)
S_2	28 881 (0.042)	25 074 (0.014)
S_3	29 740 (0.029)	29 912 (0.038)
S_4	32 942 (0.147)	33 154 (0.003)

[a] Calculated oscillator strengths are listed in parentheses. The AM1 geometry was used.

In addition, the excited-state properties of ketenimines **A** and **B** have been predicted by the INDO/S method and are presented in Table 5. The calculated (vertical) $S_0 \rightarrow S_1$ transition energy (18 953 cm^{-1}) of $C_{10}F_7N$ (**B**) is similar to the (0,0) transition frequency of 17 300 cm^{-1} of the species formed on annealing the matrix. The $S_0 \rightarrow S_1$ energy separation (20 805 cm^{-1}) of $C_{10}F_7N$ (**A**) is greater than the experimental value. Although assignment of the second species to ketenimine **B** appears consistent with the calculations presented in Table 5, it is an unreasonable assignment based on the calculated PES, as ketenimine **A** is ~10 kcal/mol more stable than its isomer **B** (Figure 8). And as mentioned above, formation of isomer **B** would require passage over an activation barrier of >20 kcal/mol.

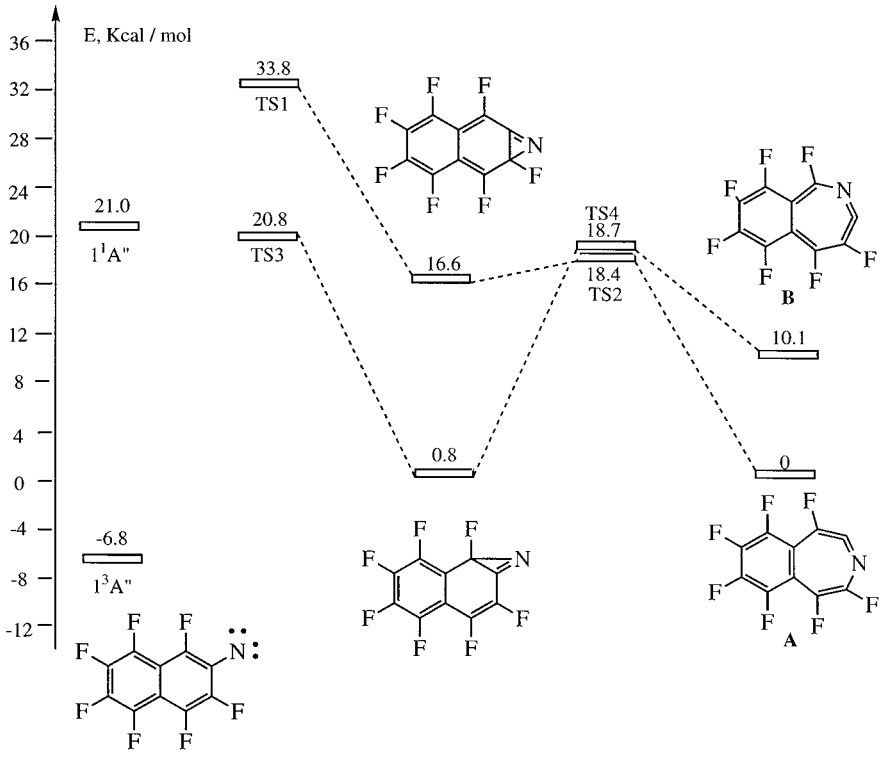

Figure 8. Potential energy surface of PFNN ($C_{10}F_7N$) and related species calculated by the B3LYP/6-31G(d) method.

TABLE 6: Comparison of Excitation Energies (cm^{-1}) from the Ground Electronic State to Four Electronically Excited States of Perfluoro-2-naphthyl Aminyl Radical PFNNH ($C_{10}F_7NH$)[a]

states	INDO/S cm^{-1} (osc. str.)	exptl (this work) cm^{-1} (adiabatic)
D_0		
D_1	15 863 (0.005)	17 300
D_2	19 636 (0.002)	
D_3	19 879 (0.005)	
D_4	23 712 (0.032)	
D_5	26 762 (0.078)	

[a] Calculated oscillator strengths are listed in parentheses. The AM1 geometry was used. The experimental value is the average of the experimental transition energy (0,0) which was observed in this work.

TABLE 7: Vertical Excitation Energies (cm^{-1}) from the Ground Electronic State to Five Electronically Excited States of 2-Naphthyl Aminyl Radical ($C_{10}H_7NH$) Using the INDO/S Method[a,b]

states	INDO/S, cm^{-1} (eV)	oscillator strength, *f*	exptl, cm^{-1} (eV)
D_0			
D_1	16 867 (2.09)	0.003	16 143 (2.0)
D_2	21 292 (2.64)	0.003	21 778 (2.7)
D_3	21 503 (2.67)	0.006	
D_4	25 316 (3.14)	0.029	24 198 (3.0)
D_5	27 793 (3.44)	0.049	26 618 (3.3)

[a] The optimized AM1 geometry was used. [b] The experimental vertical transition energies are from ref 20.

Thus, it seems more likely that the new intermediate observed upon annealing PFNN is the aryl aminyl radical produced by a hydrogen transfer reaction from the matrix host.

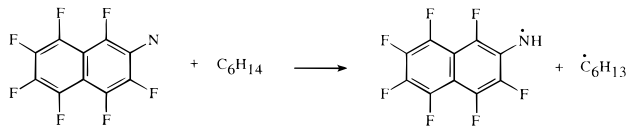

The (vertical) electronic spectra of the perfluoro-2-naphthylaminyl and the parent 2-naphthylaminyl radicals were calculated by the INDO/S method (Tables 6 and 7, respectively). The INDO/S method accurately predicts the lowest energy transition (theory 16 867, cm^{-1}; experiment, 16 143 cm^{-1}) of the parent 2-naphthylaminyl radical, as reported by Leyva et. al.[23]

The reasonable correspondence between theory and experiment with the parent 2-naphthylaminyl radical, the similar energies of the transitions of the parent and fluorinated aryl aminyl radical (experiment 17 300 cm^{-1}), and the satisfactory prediction of theory with 2-$C_{10}F_7NH^{\bullet}$ (theory, 15 863 cm^{-1}) with experiment convinces us to assign the 17 300 cm^{-1} band to the fluorinated aryl aminyl radical.

Zhai and Platz[7] reported that triplet PFNN (in a glassy organic matrix at 77 K) has three absorption bands at low energy at 546, 599, and 651 nm (18 200, 16 700, and 15 400 cm^{-1}, respectively). This is not consistent with the finding of this work that the (0,0) band of ^{3}PFNN is at 18 800 cm^{-1}. Thus, there is some discrepancy between the earlier work[7] and these efforts. Perhaps some of the absorption bands discovered by Zhai and Platz originate from the perfluoro-2-naphthylaminyl radical produced after hydrogen atom abstraction reactions of ^{3}PFNN (inadvertently irradiated along with the azide precursor) with the glassy matrix.

Vibrational Frequencies. An analysis of the vibrational frequencies listed in Tables 1 and 2 clearly indicates that similar frequencies are observed for PFNN in all matrixes studied and that slightly different frequencies are observed for the species identified with perfluoro-2-naphthylaminyl radical. The frequency of 287−297 cm^{-1} of the main vibrational compounds of PFNN is shifted to 301−305 cm^{-1} in the matrixes studied for the radical. The frequency of 387−397 cm^{-1} is characteristic of the radical. The frequencies of 1373 and 1590 cm^{-1} in the fluorescence spectra of PFNN have their corresponding frequencies at 1341−1367 and 1615−1626 cm^{-1}, respectively, in the radical. This observation provides a convincing argument that both emissions (with (0,0) origins at 18 280 and at 17 300 cm^{-1}) originate from chemically different compounds, i.e., perfluoro-2-naphthyl nitrene and perfluoro-2-naphthyl aminyl radical, respectively. By the same reasoning, the possibility that the emission assigned to the aminyl radical can be assigned to the emission originating from the T_1 state of PFNN can be excluded.

Finally, let us mention that we also tried to identify the products of the photolysis of 2-naphthyl azide in *n*-hexane at 5 K. Unfortunately, we observed only a weak emission which disappeared with time. This species had a (0,0) transition at 16 805 cm^{-1}, and therefore, it is assigned to the fluorescence of the 2-naphthyl aminyl radical. This observation is consistent with previous conclusions that polyfluorination of the aromatic ring raises the barrier to molecular rearrangement, thus making possible the spectroscopic studies of nitrenes.[6,7]

IV. Conclusions

Photolysis of perfluoro-2-naphthyl azide in low temperature (5 K) Shpolskii matrixes results in the formation of a triplet nitrene. This nitrene is persistent at low temperatures as long as the matrix is frozen. Annealing a matrix containing a nitrene leads to hydrogen atom abstraction from the surrounding matrix to create an aminyl radical, which is persistent at low temperatures. To obtain a consistent theoretical description of the experimental results, we must assume that the fluorescence of the nitrene and the aminyl radical originate from the first excited state, T_1 in the nitrene and D_1 in the aminyl radical.

Acknowledgment. Support of this work by the National Science Foundation (C.M.H. CHE-9733457) is gratefully acknowledged. C.M.H. also acknowledges support by the Ohio Supercomputer Center in a generous allocation of computer time (PAS-925) and to the donors of the Petroleum Research Fund, administered by the American Chemical Society, for partial support of this research. We are grateful for helpful discussions with Professor Matt Platz (Ohio State University). Z.Z. thanks Prof. T. Bally (University of Fribourg) for allowing us to use the MOLCAS program on his computer system. The authors are indebted to Professor Bally for stimulating discussion and many helpful comments on this manuscript.

References and Notes

(1) (a) See: Platz, M. S. In *Azides and Nitrenes, Reactivity and Utility*; Scriven, E. F. V., Ed.; Academic Press: New York, 1984. (b) Schuster, G. B.; Platz, M. S. *Adv. Photochem.* **1992**, *17*, 69.

(2) See: Breslow, D. In *Azides and Nitrenes, Reactivity and Utility*; Scriven, E. F. V., Ed.; Academic Press: New York, 1984; p 491.

(3) Bayley, H. *Photogenerated Reagents in Biochemistry and Molecular Biology*; Elsevier: New York, 1983.

(4) (a) Gritsan, N. P.; Yuzawa, T.; Platz, M. S. *J. Am. Chem. Soc.* **1997**, *119*, 5059. (b) Born, R.; Burda, C.; Senn, P.; Wirz, J. *J. Am. Chem. Soc.* **1997**, *119*, 5061.

(5) (a) Marcinek, A.; Platz, M. S.; Chan, S. Y.; Floresca, R.; Rajagopalan, K.; Golinski, M.; Watt, D. *J. Phys. Chem.* **1994**, *98*, 412. (b) Gritsan, N. P.; Zhai, H. B.; Yuzawa, T.; Karweik, D.; Brooke, J.; Platz, M. S. *J. Phys. Chem. A* **1997**, *101*, 2833.

(6) (a) Leyva, E.; Platz, M. S. *Tetrahedron Lett.* **1985**, *26*, 2147. (b) Leyva, E.; Platz, M. S.; Persy, G.; Wirz, J. *J. Am. Chem. Soc.* **1986**, *108*, 3783. (c) Hayes, J. C.; Sheridan, R. S. *J. Am. Chem. Soc.* **1990**, *112*, 5879. (d) For references of Shpolskii matrixes, see: Migirdicyan, E.; Kozankiewicz, B.; Platz, M. S. *Adv. Carbene Chem.* **1998**, *2*, 97.

(7) Zhai, H. B.; Platz, M. S. *J. Phys. Chem.* **1996**, *100*, 9568.

(8) Dunkin, I. R.; Thomson, P. C. P. *J. Chem. Soc., Chem. Commun.* **1982**, 1192.

(9) Kim, S. J.; Hamilton, T. P.; Schaefer, H. F., III *J. Am. Chem. Soc.* **1992**, *114*, 5349.

(10) (a) Hrovat, D. A.; Waali, E. E.; Borden, W. T. *J. Am. Chem. Soc.* **1992**, *114*, 8698. (b) Karney, W. L.; Borden, W. T. *J. Am. Chem. Soc.* **1997**, *119*, 1378. (c) Karney, W. L.; Borden, W. T. *J. Am. Chem. Soc.* **1997**, *119*, 3347.

(11) (a) Abramovitch, R. A.; Challand, S. R.; Yamada, Y. J. *J. Org. Chem.* **1975**, *40*, 1541. (b) Banks, H. E.; Sparkes, G. R. *J. Chem. Soc., Perkin Trans.* **1972**, *1*, 1964. (c) Haszeldine, R. N.; Parkinson, A. R.; Birchall, J. M. U.S. Patent 3,238, 1966. (d) Banks, R. E.; Sparks, G. R. *J. Chem. Soc., Perkin 1* **1972**, 1964.

(12) *Hyperchem*, release 4.5 for Windows, Moleculer Modeling System, Hypercube, Inc., 1995.

(13) Frisch, M. J.; Trucks, G. W.; Schlegel, H. B.; Gill, P. M. W.; Johnson, B. G.; Robb, M. A.; Cheeseman, J. R.; Keith, T.; Petersson, G. A.; Montgomery, J. A.; Raghavachari, K.; Al Laham, M. A.; Zakrzewski, V. G.; Ortiz, J. V.; Foresman, J. B.; Peng, C. Y.; Ayala, P. Y.; Chen, W.; Wong, M. W.; Andres, J. L.; Replogle, E. S.; Gomperts, R.; Martin, R. L.; Fox, D. J.; Binkley, J. S.; Defrees, D. J.; Baker, J.; Stewart, J. J. P.; Head-Gordon, M.; Gonzalez, C.; Pople, J. A. *Gaussian 94*; Gaussian, Inc.: Pittsburgh, PA, 1995.

(14) (a) Dewar, M. J. S.; Zoebsh, E. W.; Haels, E. E.; Stewart, J. J. P. *J. Am. Chem. Soc.* **1985**, *107*, 3902. (b) Dewar, M. J. S. *J. Mol. Struct.* **1985**, *100*, 41. (c) *AMPAC package*; Dewar Research group, University of Texas: Austin, Texas.

(15) (a) Zerner, M. C.; Ridley, J. E. *Theor. Chim. Acta* **1973**, *32*, 111. (b) Edwards, W. D.; Zerner, M. C. *Theor. Chim. Acta* **1987**, *72*, 347.

(16) Andersson, K.; Blomberg, M. R. A.; Fulscher, M. P.; Karlstrom, G.; Kello, V.; Lindh, R.; Malmqvist, P.-A.; Noga, J.; Olsen, J.; Roos. B. O.; Sadlej, A. J.; Siegbahn, P. E. M.; Urban, M.; Widmark, P.-O. *MOLCAS 4*; University of Lund: Sweden.

(17) (a) Becke, A. D. *J. Chem. Phys.* **1992**, *98*, 1372. (b) Lee, C.; Yang, W.; Parr, R. G. *Phys. Rev. B* **1988**, *37*, 785. (c) Labanowski, J. W.; Andzelm, J. *Density Functional Methods in Chemistry*; Springer: New York, 1991. (d) Parr, R. G.; Yang, W. *Density Functional Theory in Atoms and Molecules*; Oxford University Press: New York, 1989.

(18) Gritsan, N. P.; Zhu, Z.; Hadad, C. M.; Platz, M. S. *J. Am. Chem. Soc.* **1999**, *121*, 1202−1207.

(19) Després, A.; Lejeune, V.; Migirdicyan, E.; Platz, M. S. *J. Phys. Chem.* **1992**, *96*, 2486.

(20) (a) Calculated B3LYP/6-31G(d) vibrational frequencies for ketenimine **A** (unscaled, cm^{-1}) are 62.2, 76.4, 123.9, 133.9, 158.3, 172.6, 189.7, 266.4, 271.3, 281.6, 291.6, 306.6, 319.4, 341.5, 352.5, 390.5, 424.5, 445.5, 460.8, 494.6, 500.0, 524.9, 545.5, 583.4, 606.6, 658.4, 668.4, 686.9, 698.3, 781.4, 832.6, 914.4, 1043.6, 1105.8, 1160.4, 1238.3, 1256.6, 1322.2, 1335.6, 1360.7, 1384.7, 1418.9, 1502.6, 1549.3, 1614.9, 1647.8, 1667.7, and 1959.2. (b) Calculated B3LYP/6-31G(d) vibrational frequencies for ketenimine **B** (unscaled, cm^{-1}) are 59.5, 71.2, 114.0, 135.0, 157.5, 177.1, 193.6, 269.5, 279.1, 282.5, 294.7, 317.0, 318.9, 347.5, 369.2, 380.7, 418.8, 429.8, 457.3, 463.4, 514.4, 525.0, 543.4, 579.7, 603.0, 656.4, 666.0, 689.9, 709.8, 784.1, 837.7, 924.1, 1044.9, 1103.2, 1150.7, 1247.8, 1260.6, 1320.0, 1333.9, 1341.4, 1388.8, 1418.1, 1499.2, 1549.2, 1587.5, 1640.3, 1663.2, and 1784.3. (c) Calculated B3LYP/6-31G(d) vibrational frequencies for the perfluorinated aryl aminyl radical (unscaled, cm^{-1}) are 66.8, 74.9, 112.3, 138.0, 160.3, 178.1, 195.0, 270.9, 275.6, 283.6, 297.5, 308.9, 324.5, 335.1, 336.6, 369.3, 392.7, 393.8, 420.7, 448.5, 506.0, 507.2, 526.4, 539.2, 554.5, 584.9, 608.5, 647.8, 743.7, 770.2, 805.8, 816.0, 961.1, 1047.7, 1108.5, 1154.5, 1258.7, 1261.6, 1270.5, 1310.1, 1342.1, 1391.0, 1410.2, 1459.8, 1493.6, 1523.6, 1559.8, 1601.9, 1664.5, 1693.0, and 3439.4.

(21) Although the DFT methods used in this work cannot treat an open-shell singlet nitrene, they allow us to evaluate the energy change of the rearrangement reaction based on Karney and Borden's calculations (ref 10b) which showed the ketenimine and singlet PN were similar in energy.

(22) Morawietz, J.; Sander, W. *J. Org. Chem.* **1996**, *61*, 4351

(23) Leyva, E.; Platz, M. S.; Niu, B.; Wirz, J. *J. Phys. Chem.* **1987**, *91*, 2293.